Fabrication of highly porous and micropatterned SnO_2 films by oxygen bubbles generated on the anode electrode

Eiji Hosono,[ab] Shinobu Fujihara,[c] Hiroaki Imai,[c] Itaru Honma[a] and Haoshen Zhou*[ab]

Received (in Cambridge, UK) 3rd February 2005, Accepted 17th March 2005
First published as an Advance Article on the web 4th April 2005
DOI: 10.1039/b501579k

The fabrication process of highly porous SnO_2 thick film by reaction between tin ions and oxygen gas generated by an anodic applied potential on substrates in $SnCl_2$ aqueous solution is reported; moreover, we succeeded in forming porous SnO_2 micropatterns through site-selective deposition on a Pt-patterned F-doped SnO_2 (FTO) coated substrate.

Tin oxide (SnO_2) is an n-type semiconductor with a direct band gap of 3.8 eV. Nanoscale porous structures of SnO_2 with a high surface area have been required for electrochemical materials, including chemical sensors,[1] lithium ion batteries,[2] and capacitors.[3]

Direct deposition methods in a chemical bath have been investigated.[4,5] Chemical bath deposition (CBD), in which water is typically used as a solvent, have been utilized for preparing various kinds of metal oxides because thin-film materials can be fabricated at low temperatures without the expensive and special apparatus required for vapor-phase techniques. However, this method is not suitable for industry because it takes many hours for the deposition of metal oxide due to the strict control of degrees of super-saturation, which is a most important point for heterogeneous nucleation of metal oxides. Therefore, recently, electrochemical deposition has been studied. Metal oxides such as ZnO[6] and SnO_2[7]are deposited on the cathode electrode for a short time. In this system, nitrate ions are used as the oxygen source. Then metal oxides are formed through the reaction as follows: the hydroxyl groups formed on the electrode convert metal ions into metal hydroxides or metal oxides.

$$NO_3^- + H_2O + 2e^- \rightarrow NO_2^- + 2OH^-$$

$$M^{n+} + nOH^- \rightarrow M(OH)_n \rightarrow MO_{n/2} + n/2H_2O$$

This mechanism is similar to that of CBD, which is related to control of pH by addition of acid or base.

Other electrochemical deposition is conducted on the anode electrode. Chigane *et al.* reported the fabrication of MnO_x[8] by anodic electrolysis based on the potential–pH diagram[9] for a manganese–water system by Pourbaix. A report of the fabrication of porous SnO_2 on the anode electrode is an example of the anodic oxidation of tin plate.[10] As an example of the method of deposition onto the substrate, Hyde *et al.* reported nanofilm deposition of porous SnO_2 on boron-doped diamond by sonochemically assisted anodic electrochemical deposition from Sn^{2+} solution.[11]

In our previous work, SnO_2 films, which were fabricated by chemical bath deposition, were deposited by some dissolved oxygen in the solution with control of the metal concentration, pH and temperature.[12] In this paper, we paid attention to the reactivity of tin ions to oxygen. A novel process for the fabrication of highly porous SnO_2 film by reaction between tin ions and oxygen gas generated by anodic applied potential on substrates in $SnCl_2$ aqueous solution is reported. This method can be called electrochemical assisted chemical bath deposition, rather than electrochemical deposition, because the SnO_2 is formed not by oxidation potential but by oxygen gas. The resultant SnO_2 film is characterised by a porous structure with the pores being of nano/micrometre size, which are derived from gas bubbles. This structure is very useful for both battery electrode devices and gas sensor devices because these devices need the nano-scale pores for reaction sites and the micrometre-scale pores for gas or liquid transportation. Moreover, we succeeded in forming porous SnO_2 micrometre-scale patterns through site-selective deposition on F-doped SnO_2 (FTO) substrate coated Pt pattern.

Precursor solution was prepared by dissolving $SnCl_2{\cdot}2H_2O$ (99.9% purity, Wako Pure Chemicals Co., Ltd., Japan) in H_2O with the addition of HCl (99.9% purity, Wako Pure Chemicals Co., Ltd., Japan), which was added dropwise to the solution to adjust the pH value (about 0.9). The concentration of the tin ions was fixed to 0.15 mol dm^{-3}.

The cell for deposition was a conventional three electrode cell in which a Pt (200 nm)/Ti/Si plate was used as the counter electrode, separated from the working electrode of Pt (200 nm)/Ti/Si or F-doped SnO_2 coated glass substrate for SnO_2 deposition by 0.5 cm. An SCE electrode was used as the reference electrode. A constant potential was applied to the substrate in precursor solution. The morphology was observed by field emission scanning electron microscopy (FESEM) at 10 kV and high resolution transmission electron microscopy (HRTEM) at 200 kV with a Carl Zeiss Gemini Supra and a Philips TECNAI F20 microscope, respectively. The camera length for the electron diffraction (ED) pattern was 350 mm.

Fig. 1 shows the ED pattern of the film that was deposited on the Pt substrate at +2.0 V for 10 min. The clear Debye–Scherrer rings indicate that the film is composed of polycrystalline SnO_2 grains (JCPDS No. 41-1445). XRD analysis could not detect the diffraction pattern of SnO_2. It is considered that the deposited SnO_2 films are composed of very small nanoparticles.

Fig. 2A(a, b) shows the current–potential curves of the (a) Pt or (b) FTO coated substrate. The anodic currents based on the drastic formation of oxygen gas in (a) and (b) are generated at around +1.7 V and +2.5 V, respectively. The drastic difference between the current generation potentials of (a) and (b) was caused by the difference in the resistivity of the substrate (Pt: 0.1 Ω $square^{-1}$,

*hs.zhou@aist.go.jp

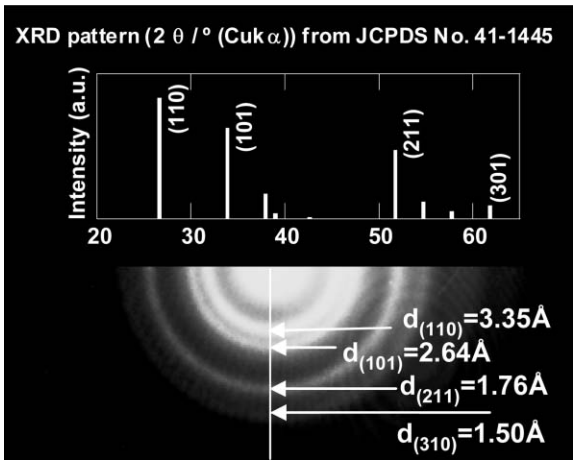

Fig. 1 Identification of the deposited film. The *d*-spacing derived from the electron diffraction pattern of the film, which was fabricated by deposition on the Pt substrate at +2.0 V (*vs.* SCE) for 10 min, indicates that the film is polycrystalline SnO_2.

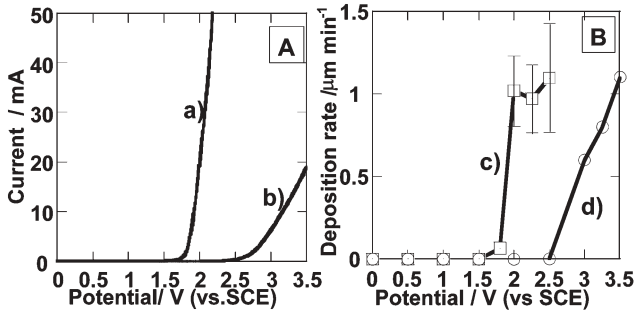

Fig. 2 Correlation between the applied potential, the generated current, and deposition rate of the films. A: The dependence of the generated current on the potential applied to a Pt electrode (a) and a FTO electrode (b); scanning rate: 20 mV s^{-1}. B: Relationship between the applied potential and deposition rate of the films on the Pt electrode (c), on the FTO electrode (d).

FTO: 10 Ω square^{-1}). Fig. 2B(c, d) indicates the relationship between the applied potential and the rate of deposition. When the potential applied to the Pt and FTO substrates was lower than the oxygen generation potential as shown in Fig. 2A(a, b), we could not confirm the deposition of SnO_2 after 10 min in the solution. In the cases using the FTO substrate, applied potentials of 2.0 V and 2.5 V for 10 min caused the formation of light scattering grains of about 10 and 20 nm in size on the FTO surface, respectively. Then, with increasing the applied potential from 3.0 to 3.5 V, the deposition rate was increased. In the same way, an increase in the applied potential from 1.8 to 2.0 V to the Pt substrate caused an increase in the deposition rate. These increases in the deposition rate are based on an increase in the amount of oxygen gas generated, as shown in Fig. 2A(a, b). However, the large increase in the potential applied to the Pt substrate (2.25 and 2.5 V) does not result in an increase in the deposition rate due to a preference for tin metal deposition at the counter electrode. Moreover, in these cases, the reproducibility of the film formation is very low due to scratching of the Pt substrate by drastic oxygen formation. The above deposition process can be classified into three groups. The first range is a very small current range. In this range, we cannot confirm the formation of the films from SEM, but it is considered that a nanofilm is formed by sonochemically assisted electrochemical deposition.[11] The second range is the range of SnO_2 formation on the anode substrate, in which the rate of deposition is increased by increasing the applied potential due to an increase in the amount of oxygen gas generated. At this time, tin metal was deposited on the cathode counter electrode. A competitive reaction between SnO_2 deposition on the anode electrode and tin deposition on the cathode electrode occurred. Third range is the range preferring tin deposition. The rate of SnO_2 deposition is not increased by an increase in the applied potential as shown in Fig. 2B(c). In other words, this range is the range of saturated deposition rate. When the FTO substrate is used as shown in Fig. 2A(b) and 2B(d), the system does not reach this range because the generated current and the rate of deposition are smaller than those in the case of using Pt substrate in Fig. 2A(a) and 2B(c).

When the applied potential on both substrates was increased, the rate of deposition increased. In other words, an increase in the oxygen gas generation rate caused the increase in the deposition rate. These results and the agreement of the plots shown in Fig. 2A and Fig. 2B indicate that SnO_2 is formed by reaction between Sn^{2+} and oxygen gas as follows, which are same reactions as in our previous work using the chemical bath deposition method.[12]

$$2H_2O \rightarrow 2H_2\uparrow + O_2\uparrow$$

$$Sn^{2+} + \tfrac{1}{2}O_2 + 3H_2O \leftrightarrow Sn(OH)_4 + 2H^+$$

$$Sn(OH)_4 + Sn(OH)_4 \leftrightarrow Sn_2O(OH)_6 + H_2O \leftrightarrow 2SnO_2 + 4H_2O$$

The equations do not contain the electrochemical reaction. The electrode potential is very positive, hence, the likeliest explanation is that Sn(II) is simply being electrochemically oxidized to Sn(IV). However, if electrochemical oxidation from Sn(II) to Sn(IV) occurred, the hollow morphology observed (Fig. 3) would not be obtained because the hollow morphology could be obtained by oxygen bubble morphology. The morphology of electrochemical oxidization is not the bubble-like morphology.

The SEM (a, b) and TEM (c, d) images of the prepared films deposited on the Pt substrate for 10 min at +2.0 V are shown in Fig. 3. We can see porous morphology with spherical nanosized pores and micrometre-scale pores. It is considered that nano-scale pores are created by nano bubbles, which are formed at the early stage of gas generation, and micrometre-scale pores are created by micrometre-scale bubbles formed by coalescence of nano bubbles. The reaction at the gas/liquid interface, results in nano- and micrometre-scale hollow spheres. The fabrication of a porous structure by electrochemical deposition with formed H_2 bubbles has been reported by H. Chin *et al.*[13] In this present case, oxygen gas bubbles are used as both the reaction agent for oxidation and the template of the porous structure. From the images of (c) and (d), the thickness of the walls, which construct the nanopore, is about 20 nm. This thickness agrees with that of the SEM images as shown in (b). We can see crystallized particles with a grain size of 2.5 nm from high magnification images of (d). A lattice image due to phase contrast corresponds to the interplanar distance of SnO_2 (110) with $d_{(110)}$ = 3.35 Å. The specific surface area was calculated

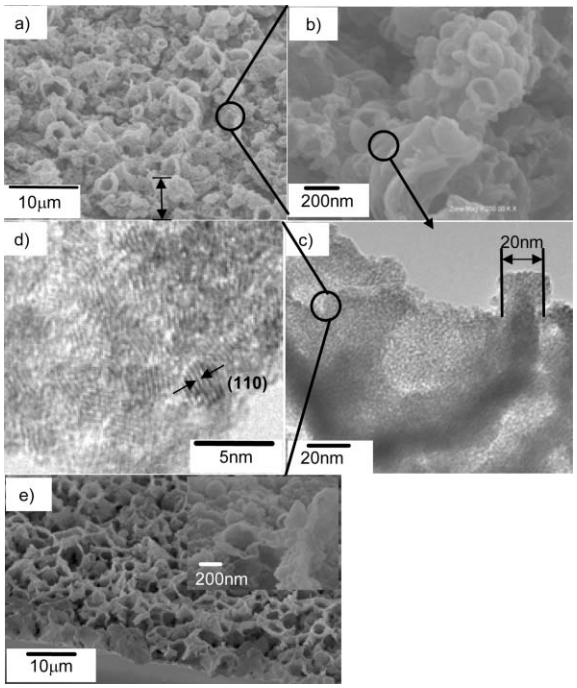

Fig. 3 Morphology of the deposited films. SEM (a, b) and TEM (c, d) images of the films fabricated by the deposition on Pt substrate at +2.0 V (*vs.* SCE) for 10 min shows highly porous morphology and nano-walls constructed of nanocrystalline SnO_2, respectively. SEM images of the film (e) fabricated by the deposition on FTO substrate at +3.0 V (*vs.* SCE) for 10 min indicate similar morphology to the film on the Pt substrate.

by BET methods, on the basis of N_2 adsorption and desorption isotherms at 77 K. The BET surface area of the film deposited on the Pt substrate at +2.0 V for 10 min after deposition is 120 $m^2\ g^{-1}$. The high surface area is derived from the existence of nanometre-sized pores from TEM images. SEM images of the prepared films deposited on the FTO substrate for 10 min at +3.0 V are shown in Fig. 3(e). The morphology is similar to that on the Pt substrate. This result indicates that the porous SnO_2 films with nano- and micrometre-scale pores are fabricated on the electro-conductive materials. These films were never taken off by surface tension on drying. However, the scratch hardness is low because the porous morphology is constructed by the nano-walls about 20 nm thick.

Fig. 4 shows the SEM images of the patterned porous SnO_2 film. Firstly, Pt was sputtered on the FTO with 400 mesh Cu (Okenshoji Co., Ltd). The deposition was conducted on the Pt-patterned FTO as working electrode at 2.0 V for 3 min. We can see clearly patterned films. The images of the non-Pt coated (c) and Pt coated (d) parts show the bare FTO surface and porous SnO_2, respectively. When we used Au-patterned FTO, a similar porous SnO_2 pattern was obtained. Therefore, it is considered that the catalytic effect of Pt does not participate. From Fig. 2B, the +2.0 V potential applied to the FTO substrate caused almost no deposition of porous SnO_2 films due to the low current produced by the small amount of generated O_2 gas. It is considered that the parts of the film labelled (c) and (d) in Fig. 4 correspond to the first and second ranges of the deposition process, as mentioned above, respectively. Therefore, oxygen gas is generated preferentially on Pt rather than on FTO. As a result, patterned porous film was obtained according to patterned Pt.

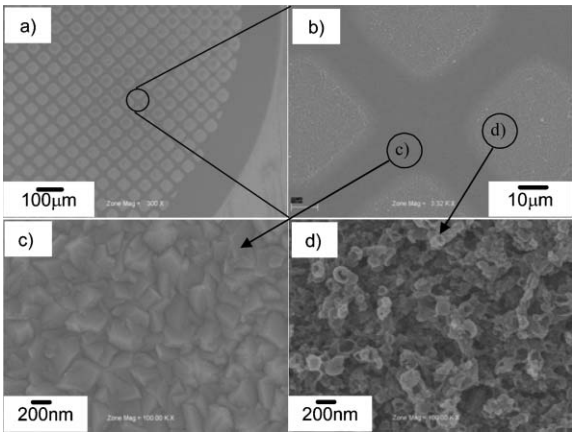

Fig. 4 The images of the micropatterned SnO_2 films. SEM images of the film fabricated by deposition on the Pt patterned FTO substrate at +2.0 V (*vs.* SCE) for 3 min. The images (a) and (b) shows the micropatterned films. The non-Pt coated parts are bare FTO surface (c). Porous SnO_2 is deposited on the Pt coated parts (d).

In conclusion, we fabricated porous SnO_2 film and patterned film by the electrochemical assisted CBD method, which is based on the reaction between tin ions and oxygen gas generated by electrochemical reaction. We believe this fabrication strategy will open an avenue for production of pattern controlled nano- and micrometre-scale porous metal oxide films of other metals.

Eiji Hosono,[ab] Shinobu Fujihara,[c] Hiroaki Imai,[c] Itaru Honma[a] and Haoshen Zhou*[ab]

[a]*National Institute of Advanced Industrial Science and Technology, Umezono, 1-1-1, Tsukuba 305-8568, Japan. E-mail: hs.zhou@aist.go.jp; Fax: 81-298-61-5799; Tel: 81-298-61-5795*

[b]*Japan Science and Technology, PRESTO, Kawaguchi, Saitama 332-0012, Japan*

[c]*Keio University, 3-14-1, Hiyoshi, Kohoku-ku, Yokohama 223-8522, Japan*

Notes and references

1 N. S. Baik, G. Sakai, N. Miura and N. Yamazoe, *Sens. Actuators, B*, 2000, **63**, 74–79.
2 Y. Idota, T. Kubota, A. Matsufuji, Y. Maekawa and T. Miyasaka, *Science*, 1997, **276**, 1395–1397.
3 N. L. Wu, J. Y. Hwang, P. Y. Liu, C. Y. Han, S. L. Kuo, K. H. Liao, M. H. Lee and S. Y. Wang, *J. Electrochem. Soc.*, 2001, **148**, A550–A553.
4 B. C. Bunker, P. C. Rieke, B. J. Tarasevich, A. A. Campbell, G. E. Fryxell, G. L. Graff, L. Song, J. Liu, W. Virden and G. L. McVay, *Science*, 1994, **264**, 48–55.
5 T. P. Niesen and M. R. De Guire, *J. Electroceram.*, 2001, **6**, 169–207.
6 M. Izaki and T. Omi, *J. Electrochem. Soc.*, 1997, **144**, 1949–1952.
7 S. T. Chang, I. C. Leu and M. H. Hon, *Electrochem. Solid State Lett.*, 2002, **5**, C71–C75.
8 M. Chigane and M. Ishikawa, *J. Electrochem. Soc.*, 2000, **147**, 2246–2251.
9 M. Pourbaix, in *Atlas of Electrochemical Equilibria in Aqueous Solutions*, Pergamon Press, Brussels, 1996, p. 286.
10 H. C. Shin, J. Dong and M. L. Liu, *Adv. Mater.*, 2004, **16**, 237–240.
11 M. Hyde, A. J. Saterlay, S. J. Wilkins, J. S. Foord, R. G. Compton and F. Marken, *J. Solid State Electrochem.*, 2002, **6**, 183–187.
12 H. Ohgi, T. Maeda, E. Hosono, S. Fujihara and H. Imai, *Cryst. Growth Des.*, 2005 (DOI: 10.1021/cg049644z).
13 H. C. Shin, J. Dong and M. L. Liu, *Adv. Mater.*, 2003, **19**, 1610–1614.